Light transport in three-dimensional semi-infinite scattering media

André Liemert and Alwin Kienle*

Institut für Lasertechnologien in der Medizin und Meßtechnik, Helmholtzstrasse12, D-89081 Ulm, Germany
**Corresponding author: alwin.kienle@ilm.uni-ulm.de*

Received March 6, 2012; revised April 23, 2012; accepted May 7, 2012;
posted May 8, 2012 (Doc. ID 164302); published June 29, 2012

The three-dimensional radiative transfer equation is solved for modeling the light propagation in anisotropically scattering semi-infinite media such as biological tissue, considering the effect of internal reflection at the interfaces. The two-dimensional Fourier transform and the modified spherical harmonics method are applied to derive the general solution to the associated homogeneous problem in terms of analytical functions. The obtained solution is used for solving boundary-value problems, which are important for applications in the biomedical optics field. The derived equations are successfully verified by comparisons with Monte Carlo simulations.

OCIS codes: 170.3660, 010.5620, 000.3860.

1. INTRODUCTION

The radiative transfer equation (RTE) is involved in many areas of physics to model the propagation of waves in random scattering media such as in astronomy, neutron transport, heat transfer, computer graphics, and climate research [1–3]. In the field of biomedical optics, the RTE is considered to be the gold standard both for therapeutic and diagnostic applications. Because of the lack of analytical solutions of the RTE for relevant geometries, numerical methods or approximative equations were considered. The Monte Carlo method was mostly used as numerical solution of the RTE [4–6], but other techniques like the finite element [7], the finite-difference [8], or the discrete-ordinate method [9] were also applied. For the isotropic scattering case, Williams [10] solved the RTE for the semi-infinite geometry with internal reflection. Recently, analytical solutions for the steady-state RTE were obtained for unbounded anisotropically scattering media [11,12] and the slab geometry [13,14]. In this study we derived the solution to the boundary-value problem in the semi-infinite geometry including, for the first time to our knowledge, its successful validation by comparison with Monte Carlo simulations. Additionally, we considered mismatched boundary conditions (BCs) by implementing Fresnel reflection.

The paper is divided into the following sections. In Subsection 2.A, an analytical expression for the general solution to the homogeneous RTE is derived similar to what was recently accomplished for the two-dimensional case [15,16]. To this end, we make use of the method of rotated reference frames that was developed by the authors of the publications [11,13,14]. In Subsection 2.B, the obtained homogeneous solution is applied for solving the boundary-value problem in the semi-infinite geometry considering internal and external sources. In Section 3, the derived general solution is verified by comparing the reflectance, the fluence, and the radiance with Monte Carlo simulations. In support of the implementation of the derived equations, we included the numerical procedure for obtaining the general solution to the homogeneous RTE in Appendix A.

2. THEORY

A. General Solution to the Homogeneous RTE

In this section, the general solution to the homogeneous RTE is derived for solving the boundary-value problem in the semi-infinite geometry. The three-dimensional homogeneous RTE for the radiance $\psi(\mathbf{r},\hat{\mathbf{s}})$ in Cartesian coordinates is given by [1]

$$\hat{\mathbf{s}}\cdot\nabla\psi(\mathbf{r},\hat{\mathbf{s}})+\mu_t\psi(\mathbf{r},\hat{\mathbf{s}})=\mu_s\int f(\hat{\mathbf{s}}\cdot\hat{\mathbf{s}}')\psi(\mathbf{r},\hat{\mathbf{s}}')\mathrm{d}^2s', \tag{1}$$

where $\mu_t=\mu_a+\mu_s$ is the total attenuation coefficient, μ_a the absorption coefficient, and μ_s the scattering coefficient. The unit vector $\hat{\mathbf{s}}$ specifies the direction of the wave propagation, and the phase function $f(\hat{\mathbf{s}}\cdot\hat{\mathbf{s}}')$ describes the probability that a particle coming from direction $\hat{\mathbf{s}}'$ is scattered into direction $\hat{\mathbf{s}}$. In the following it is assumed that the scattering half-space medium is laterally unbounded so that the only BC regarding the coordinates (ρ,ϕ_ρ) is given by $\psi(\mathbf{r},\hat{\mathbf{s}})\to 0$ for $\rho\to\infty$. At the beginning of the derivations, the radiance is expanded by the two-dimensional Fourier integral

$$\psi(\mathbf{r},\hat{\mathbf{s}})=\frac{1}{(2\pi)^2}\int\psi(\mathbf{q},z,\hat{\mathbf{s}})\exp(\mathrm{i}\mathbf{q}\cdot\rho)\mathrm{d}^2q, \tag{2}$$

leading to a simplified version of Eq. (1) with only one spatial derivative,

$$\left[\cos\theta\frac{\partial}{\partial z}+\mathrm{i}q\sin\theta\cos(\phi-\phi_{\mathbf{q}})+\mu_t\right]\psi(\mathbf{q},z,\hat{\mathbf{s}})=\mu_s\int f(\hat{\mathbf{s}}\cdot\hat{\mathbf{s}}')\psi(\mathbf{q},z,\hat{\mathbf{s}}')\mathrm{d}^2s'. \tag{3}$$

The boundary-value problem to RTE Eq. (3) for the semi-infinite geometry can be solved by seeking solutions in form of the plane-wave mode

$$\psi(\mathbf{q},z,\hat{\mathbf{s}}) = e^{\xi z}\psi(\mathbf{q},\hat{\mathbf{s}}), \tag{4}$$

where ξ and $\psi(\mathbf{q},\hat{\mathbf{s}})$ are the unknown eigenvalue and eigenfunction, respectively. Substitution of this mode in Eq. (3) results in the eigenvalue problem

$$[\mu_t + \mathbf{k}\cdot\hat{\mathbf{s}}]\psi(\mathbf{q},\hat{\mathbf{s}}) = \mu_s \int f(\hat{\mathbf{s}}\cdot\hat{\mathbf{s}}')\psi(\mathbf{q},\hat{\mathbf{s}}')\mathrm{d}^2 s', \tag{5}$$

where $\mathbf{k}$ is a complex wave vector of the form

$$\mathbf{k} = \begin{pmatrix} \mathrm{i}q_1 \\ \mathrm{i}q_2 \\ \xi \end{pmatrix} = k\begin{pmatrix} \sin\theta_{\mathbf{k}}\cos\phi_{\mathbf{q}} \\ \sin\theta_{\mathbf{k}}\sin\phi_{\mathbf{q}} \\ \cos\theta_{\mathbf{k}} \end{pmatrix}, \tag{6}$$

with the norm $k = \sqrt{\mathbf{k}\cdot\mathbf{k}}$ and an unknown polar angle $\theta_{\mathbf{k}}$. For the further procedure, the method of rotated reference frames [11,13,14] is used to expand the eigenfunctions in terms of spherical harmonics $Y_{lm}(\hat{\mathbf{s}};\hat{\mathbf{k}})$, which are rotated by the azimuthal and polar angle of the above wave vector, yielding

$$\psi(\mathbf{q},\hat{\mathbf{s}}) = \sum_{l=0}^{\infty}\sum_{M=-l}^{l}(-1)^l \psi_{lM} Y_{lM}(\hat{\mathbf{s}};\hat{\mathbf{k}}), \tag{7}$$

where ψ_{lM} are the unknown expansion coefficients and the alternating sign is only due to convenience. Similarly, valid for the conventional spherical harmonics $Y_{lm}(\hat{\mathbf{s}}) = Y_{lm}(\hat{\mathbf{s}};\hat{\mathbf{z}})$ [17], the rotated functions satisfy the relation

$$\begin{aligned}(\hat{\mathbf{k}}\cdot\hat{\mathbf{s}})Y_{lm}(\hat{\mathbf{s}};\hat{\mathbf{k}}) = &\sqrt{\frac{l^2-m^2}{4l^2-1}}Y_{l-1,m}(\hat{\mathbf{s}};\hat{\mathbf{k}}) \\ &+ \sqrt{\frac{(l+1)^2-m^2}{4(l+1)^2-1}}Y_{l+1,m}(\hat{\mathbf{s}};\hat{\mathbf{k}}).\end{aligned} \tag{8}$$

The rotationally invariant phase function is independent on the direction of the wave vector and analogously used in the form [13]

$$f(\hat{\mathbf{s}}\cdot\hat{\mathbf{s}}') = \sum_{l=0}^{\infty}\sum_{M=-l}^{l} f_l Y_{lM}(\hat{\mathbf{s}};\hat{\mathbf{k}})Y^*_{lM}(\hat{\mathbf{s}}';\hat{\mathbf{k}}), \tag{9}$$

where the expansion coefficients are defined by

$$f_l = 2\pi\int_{-1}^{1} f(\zeta)P_l(\zeta)\mathrm{d}\zeta, \tag{10}$$

and $P_l(x)$ are the Legendre polynomials. Inserting all series in Eq. (5) and making use of relation Eq. (8) leads to the simplified block-diagonal eigenvalue problem for $M \in \mathbb{Z} \wedge l \geq |M|$:

$$k\sqrt{\frac{l^2-M^2}{4l^2-1}}\psi_{l-1,M} + k\sqrt{\frac{(l+1)^2-M^2}{4(l+1)^2-1}}\psi_{l+1,M} - \sigma_l\psi_{lM} = 0, \tag{11}$$

where $\sigma_l = \mu_a + (1-f_l)\mu_s$. Because of reasons regarding the numerical implementation of the derived solution, all series are truncated at $l = N$ with $\psi_{-1,M} = \psi_{N+1,M} = 0$, and N is always assumed as an odd number. The solution of the above block-diagonal system Eq. (11) is reducible to an eigenvalue decomposition (EVD) of N symmetric tridiagonal matrices $\mathbf{B}_M = \mathbf{B}_{-M}$ for the values $M = 0,1,\ldots,N-1$, which have the form

$$\mathbf{B}_M = \begin{pmatrix} 0 & \beta_{lM} & 0 & 0 & \cdots & 0 \\ \beta_{lM} & 0 & \beta_{l+1,M} & 0 & \cdots & \vdots \\ 0 & \beta_{l+1,M} & \ddots & \ddots & \cdots & 0 \\ 0 & 0 & \ddots & \ddots & \ddots & 0 \\ \vdots & \cdots & \cdots & \ddots & 0 & \beta_{NM} \\ 0 & \cdots & 0 & 0 & \beta_{NM} & 0 \end{pmatrix}, \tag{12}$$

where $l = M+1, M+2,\ldots,N$, and the quantities

$$\beta_{lM} = \sqrt{\frac{l^2-M^2}{(4l^2-1)\sigma_{l-1}\sigma_l}}. \tag{13}$$

Note that the special case $M = N$ leads directly to the trivial solution $\psi_{NN} = 0$. Furthermore, it can be seen that, for increasing values of M, the dimensions of the resulting block matrices $\mathbf{B}_M$ decrease where the largest value $M = N-1$ results in

$$\mathbf{B}_{N-1} = \begin{pmatrix} 0 & \beta_{N,N-1} \\ \beta_{N,N-1} & 0 \end{pmatrix}. \tag{14}$$

Every block matrix $\mathbf{B}_M$ gives $(N+1)/2 - \lceil M/2\rceil$ positive and real eigenvalues so that the EVD $\forall M = \{0,\ldots,N-1\}$ leads all in all to $(N+1)^2/4$ eigenvalues $\Lambda = \{\lambda_1,\lambda_2,\ldots\}$ with the corresponding eigenvectors $|\nu\rangle$. Here $\lceil x\rceil = \min\{k \in \mathbb{Z} | k \geq x\}$ is the ceiling function, which rounds the elements of x to the nearest integers greater than or equal to x. Note that the eigenvalues within Λ are ordered according to increasing indices of the block matrices $\mathbf{B}_M$. The EVD also delivers eigenvalues with negative sign and additionally for M odd eigenvalues that are zero. However, it can be shown that the complete set of plane-wave modes is spanned by the eigenvalues $\lambda \in \Lambda$. Upon the EVD of the above tridiagonal matrices, the solution of the block-diagonal system Eq. (11) is obtained as $\psi_{lM} = \langle l|\nu\rangle/\sqrt{\sigma_l}$, where $|M| \leq l \leq N$. Additionally, the symmetry relation of the Green's function for the radiance requires that the expansion coefficients must satisfy the condition $\psi_{l,-M} = (-1)^M\psi_{lM}$, which leads to the fact that the eigenvector components for positive and negative M are not always the same. Thus, for a fixed eigenvalue $\lambda \in \Lambda$, the corresponding eigenfunction from Eq. (7) becomes the form

$$\psi(\mathbf{q},\hat{\mathbf{s}}) = \sum_{l=M}^{N}(-1)^l\frac{\langle l|\nu\rangle}{\sqrt{\sigma_l}}[Y_{lM}(\hat{\mathbf{s}};\hat{\mathbf{k}}) + (-1)^M(1-\delta_{M0})Y_{l,-M}(\hat{\mathbf{s}};\hat{\mathbf{k}})]. \tag{15}$$

Note that there exists a function $f : \lambda \mapsto M$ that associates each eigenvalue $\lambda \in \Lambda$ for which the corresponding tridiagonal matrix is $\mathbf{B}_M$. The solution of Eq. (11) involves the dispersion

relation $k = \sqrt{\xi^2 - q^2} = 1/\lambda$, which leads to the required eigenvalues for evanescent plane-wave modes in the scattering half-space $z \geq 0$:

$$\xi = \xi(q) = -\sqrt{q^2 + \frac{1}{\lambda^2}}. \tag{16}$$

The general solution to the homogeneous RTE is completed after the evaluation of the rotated spherical harmonics in Eq. (15), which can be expanded by the linear combination [13,14]

$$Y_{lM}(\hat{\mathbf{s}}; \hat{\mathbf{k}}) = \sum_{m=-l}^{l} d^l_{mM}(\theta_{\mathbf{k}}) Y_{lm}(\theta, \phi - \phi_{\mathbf{q}}), \tag{17}$$

where $d^l_{mM}(\theta_{\mathbf{k}})$ is the Wigner d function. For the calculation of the Wigner d functions, we first determine the unknown polar angle $\theta_{\mathbf{k}}$ via comparison of the vector components in Eq. (6), yielding

$$\theta_{\mathbf{k}} = \theta_{\mathbf{k}}(q\lambda) = \arccos\left(\frac{\xi}{k}\right) = \pi - \mathrm{i}\,\mathrm{arsinh}(q\lambda). \tag{18}$$

Inserting the obtained polar angle in the closed-form expression for the Wigner d functions gives the result

$$d^l_{mM}[\theta_{\mathbf{k}}(q\lambda)] = \mathrm{i}^{M-m}\sqrt{(l+m)!(l-m)!(l+M)!(l-M)!} \times \sum_k \frac{\left[\sqrt{1+(q\lambda)^2} - 1\right]^{l-k+\frac{M-m}{2}} \left[1 + \sqrt{1+(q\lambda)^2}\right]^{k+\frac{m-M}{2}}}{2^l k!(l-m-k)!(l+M-k)!(m-M+k)!}, \tag{19}$$

where $\max\{M-m, 0\} \leq k \leq \min\{l-m, l+M\}$. The above closed-form expression can be evaluated efficiently by making use of a recursively defined algorithm reported in [18]. In Appendix A, readers will find this algorithm, including all required recurrences. Substitution of the rotation formula Eq. (17) into Eq. (15) leads to the superposition of plane-wave modes

$$\psi(\mathbf{q}, z, \hat{\mathbf{s}}) = \sum_{\lambda_i > 0} C_i(\mathbf{q}) e^{-\sqrt{q^2 + 1/\lambda_i^2} z} \sum_{l=M}^{N} \sum_{m=-l}^{l} \psi_{lm}(q\lambda_i) Y_{lm}(\theta, \phi - \phi_{\mathbf{q}}), \tag{20}$$

where

$$\psi_{lm}(q\lambda_i) = (-1)^l \frac{\langle l|\nu_i\rangle}{\sqrt{\sigma_l}} [d^l_{mM}[\theta_{\mathbf{k}}(q\lambda_i)] + (-1)^M (1 - \delta_{M0}) d^l_{m,-M}[\theta_{\mathbf{k}}(q\lambda_i)]], \tag{21}$$

and $\psi_{lm}(q\lambda_i) = 0 \,\forall\, l < M$. Remember that each eigenvalue λ_i corresponds exactly with one M. Equation (20) states the general solution to the homogeneous RTE Eq. (3) for the semi-infinite geometry.

The obtained homogeneous solution must be integrated according to Eq. (2). Further simplification regarding the inverse Fourier transform can be obtained in cases of cylindrical symmetry when the radiance only depends on the difference $\chi = \phi - \phi_\rho$. Then the constants $C_i(\mathbf{q}) = C_i(q)$ become independent of the angular variable $\phi_{\mathbf{q}}$ so that the integration regarding this variable can be performed analytically, yielding the radiance in real space

$$\psi(\mathbf{r}, \hat{\mathbf{s}}) = \sum_{l=0}^{N} \sqrt{\frac{2l+1}{4\pi}} \sum_{m=0}^{l} (2 - \delta_{m0}) \psi_{lm}(\rho, z) d^l_{m0}(\theta) \cos(m\chi), \tag{22}$$

where the kernels are given in form of an inverse Hankel transform [19],

$$\psi_{lm}(\rho, z) = \frac{\mathrm{i}^m}{2\pi} \int_0^\infty J_m(q\rho) \sum_{i=1}^{i_l} C_i(q) \psi_{lm}(q\lambda_i) e^{-\sqrt{q^2 + 1/\lambda_i^2} z} q\,\mathrm{d}q, \tag{23}$$

and $J_m(x)$ is the Bessel function of the first kind. The upper limit of the inner sum is given by

$$i_l = \frac{(N+1)(l+1)}{2} - \left\lceil \frac{l+1}{2} \right\rceil \left\lfloor \frac{l+1}{2} \right\rfloor, \tag{24}$$

where $\lfloor x \rfloor = \max\{k \in \mathbb{Z} | k \leq x\}$ is the floor function. Note that the upper limit is due to convenience for selecting only the nonzero coefficients $\psi_{lm}(q\lambda_i) \neq 0$. The final results do not change in any way if the summations are performed over all eigenvalues λ_i, which entails the limit $i_l = (N+1)^2/4 \forall l \in \{0, \ldots, N\}$.

B. Solution of Boundary-Value Problems

In this section the derived general solution to the homogeneous RTE is used for solving two different types of boundary-value problems. The semi-infinite geometry is bounded by the plane $z = 0$ with the corresponding outward normal vector $\hat{\mathbf{n}} = -\hat{\mathbf{z}}$.

1. Isotropic Point Source in the Semi-Infinite Medium

Suppose that the radiation field inside a semi-infinite medium is caused by the isotropic emitting point source $S(\mathbf{r}, \hat{\mathbf{s}}) = \delta(\boldsymbol{\rho})\delta(z - z_0)/(4\pi)$, which is located at $z = z_0$ on the positive z axis. For modeling the light propagation in the scattering half-space medium, we at first require knowledge of the radiation field in the unbounded medium, which is given by the infinite-space Green's function

$$\psi^{(p)}(\mathbf{r}, \hat{\mathbf{s}}) = \sum_{l=0}^{N} \sum_{m=-l}^{l} \psi^{(p)}_{lm}(\rho, z) Y_{lm}(\theta, \chi), \tag{25}$$

where

$$\psi^{(p)}_{lm}(\rho, z) = \frac{1}{4\pi\sqrt{\pi\sigma_0\sigma_l}} \sqrt{\frac{(l-m)!}{(l+m)!}} P^m_l\left[\frac{z - z_0}{R}\right] \times \sum_{i=1}^{\frac{N+1}{2}} \frac{\langle l|\nu_i\rangle \langle \nu_i|0\rangle}{\lambda_i^3} k_l\left[\frac{R}{\lambda_i}\right]$$

and the distance $R = \sqrt{\rho^2 + (z - z_0)^2}$. The functions $P^m_l(x)$ and $k_l(x)$ are the associated Legendre polynomials and the spherical Bessel function of the second kind, respectively. Note that the above infinite-space Green's function only contains the positive eigenvalues and the belonging eigenvectors of the tridiagonal matrix $\mathbf{B}_0$, which are labeled by the indices $i = 1, 2, \ldots, (N+1)/2$. For obtaining the corresponding Green's function in the semi-infinite medium, the RTE must be solved under the BC

$$\psi(\boldsymbol{\rho}, z=0, \hat{\mathbf{s}}) = R(\hat{\mathbf{s}}' \cdot \hat{\mathbf{n}})\psi(\boldsymbol{\rho}, z=0, \hat{\mathbf{s}}'), \qquad \hat{\mathbf{s}} \cdot \hat{\mathbf{n}} < 0, \tag{26}$$

where $R(\hat{\mathbf{s}}' \cdot \hat{\mathbf{n}})$ is the Fresnel reflection coefficient, which is defined below, and $\hat{\mathbf{s}}'$ is the mirrored unit vector of propagation characterized by the angles $\theta' = \pi - \theta$ and $\phi' = \phi$. Note that, for solving this boundary-value problem, the radiance $\psi(\mathbf{r}, \hat{\mathbf{s}}) = \psi^{(h)}(\mathbf{r}, \hat{\mathbf{s}}) + \psi^{(p)}(\mathbf{r}, \hat{\mathbf{s}})$ is considered in parts of the homogeneous solution Eq. (22) and the particular part of Eq. (25). For the further procedure, the infinite-space Green's function Eq. (25) must be expanded in plane-wave decomposition according to Eq. (2). Performing the two-dimensional Fourier transform

$$\psi^{(p)}(\mathbf{q}, z, \hat{\mathbf{s}}) = \int \psi^{(p)}(\mathbf{r}, \hat{\mathbf{s}}) \exp(-\mathrm{i}\mathbf{q} \cdot \boldsymbol{\rho}) \mathrm{d}^2\rho \tag{27}$$

yields the infinite-space Green's function in the transformed space

$$\psi^{(p)}(\mathbf{q}, z, \hat{\mathbf{s}}) = \sum_{l=0}^{N} \sum_{m=-l}^{l} \psi_{lm}^{(p)}(q, z) Y_{lm}(\theta, \phi - \phi_{\mathbf{q}}), \tag{28}$$

where

$$\psi_{lm}^{(p)}(q, z) = \frac{(-1)^l}{\sqrt{4\pi\sigma_0\sigma_l}} [\mathrm{sgn}(z - z_0)]^{l+m} \sum_{i=1}^{\frac{N+1}{2}} \times \frac{\langle l|\nu_i\rangle \langle \nu_i|0\rangle}{\lambda_i^2} \frac{e^{-\sqrt{q^2+1/\lambda_i^2}|z-z_0|}}{\sqrt{q^2 + 1/\lambda_i^2}} d_{m0}^{l}[\theta_{\mathbf{k}}(q\lambda_i)] \tag{29}$$

and the associated BC

$$\psi(\mathbf{q}, z=0, \hat{\mathbf{s}}) = R(\hat{\mathbf{s}}' \cdot \hat{\mathbf{n}})\psi(\mathbf{q}, z=0, \hat{\mathbf{s}}'), \qquad \hat{\mathbf{s}} \cdot \hat{\mathbf{n}} < 0. \tag{30}$$

Substituting the general solution in the BC Eq. (30), multiplying both sides with $Y_{l'm'}^{*}(\hat{\mathbf{s}})$, and integrating over the hemisphere $\hat{\mathbf{s}} \cdot \hat{\mathbf{n}} < 0$ results in the following set of linear equations:

$$\sum_{\lambda_i > 0} C_i(q) \sum_{l=\bar{l}}^{N} \psi_{lm'}^{(h)}(q\lambda_i) R_{l'l}^{m'} = -\sum_{l=m'}^{N} \psi_{lm'}^{(p)}(q, z=0) R_{l'l}^{m'}, \tag{31}$$

where $\bar{l} = \max\{m', M\}$ and the coefficients

$$R_{l'l}^{m'} = \frac{1}{2} \sqrt{\frac{(2l+1)(2l'+1)(l-m')!(l'-m')!}{(l+m')!(l'+m')!}} \int_0^1 [1 - (-1)^{l+m'} R(\mu)] \times P_l^{m'}(\mu) P_{l'}^{m'}(\mu) \mathrm{d}\mu. \tag{32}$$

By defining the ratio $n = n_{\mathrm{in}}/n_{\mathrm{out}}$, the Fresnel reflection coefficient can be written in the form [20]

$$R(\mu) = \frac{1}{2}\left(\frac{\mu - n\mu_0}{\mu + n\mu_0}\right)^2 + \frac{1}{2}\left(\frac{\mu_0 - n\mu}{\mu_0 + n\mu}\right)^2, \qquad \mu > \mu_c, \tag{33}$$

where $\mu_c = \sqrt{n^2 - 1}/n$ is the cosine of the critical angle, $\mu_0 = \sqrt{1 - n^2(1-\mu^2)}$, and n_{out} and n_{in} are the refractive indices outside and inside the scattering half-space, respectively. Note that, for $\mu < \mu_c$, the reflection coefficient becomes $R(\mu) = 1$.

For every value $m' = 0, 1, \ldots, N-1$, taking equations from Eq. (31) for the corresponding numbers $l' = m' + 1, m' + 3, \ldots, N$ results in $(N+1)^2/4$ linearly independent equations, which is exactly the number of unknown constants. Because of the cylindrical symmetry of the obtained solution, the homogenous part must be integrated according to the inverse Hankel transform Eq. (23).

The spatially resolved reflectance on the boundary of the semi-infinite medium is defined as

$$R(\boldsymbol{\rho}) = \int_{\hat{\mathbf{s}} \cdot \hat{\mathbf{n}} > 0} [1 - R(\hat{\mathbf{s}} \cdot \hat{\mathbf{n}})](\hat{\mathbf{s}} \cdot \hat{\mathbf{n}})\psi(\boldsymbol{\rho}, z=0, \hat{\mathbf{s}}) \mathrm{d}^2 s. \tag{34}$$

By using the BC Eq. (26), the reflectance can be also written without the Fresnel reflection coefficients

$$R(\boldsymbol{\rho}) = \int (\hat{\mathbf{s}} \cdot \hat{\mathbf{n}})\psi(\boldsymbol{\rho}, z=0, \hat{\mathbf{s}}) \mathrm{d}^2 s, \tag{35}$$

where the integration has been extended to the full unit sphere. Inserting the obtained Green's function for the semi-infinite medium in Eq. (35) leads to the rotationally symmetric reflectance

$$R(\rho) = -\sqrt{\frac{4\pi}{3}} [\psi_{10}^{(h)}(\rho, 0) + \psi_{10}^{(p)}(\rho, 0)], \tag{36}$$

where

$$\psi_{10}^{(h)}(\rho, 0) = \frac{1}{2\pi} \int_0^\infty J_0(q\rho) \sum_{i=1}^{N} C_i(q) \psi_{10}(q\lambda_i) q \mathrm{d}q. \tag{37}$$

The fluence within the semi-infinite medium is given by

$$\Phi(\mathbf{r}) = \int \psi(\mathbf{r}, \hat{\mathbf{s}}) \mathrm{d}^2 s = \sqrt{4\pi} [\psi_{00}^{(h)}(\rho, z) + \psi_{00}^{(p)}(\rho, z)], \tag{38}$$

where

$$\psi_{00}^{(h)}(\rho, z) = \frac{1}{2\pi} \int_0^\infty J_0(q\rho) \sum_{i=1}^{\frac{N+1}{2}} C_i(q) \psi_{00}(q\lambda_i) e^{-\sqrt{q^2+1/\lambda_i^2} z} q \mathrm{d}q. \tag{39}$$

2. External Incident Beam on the Semi-Infinite Medium

For modeling the light propagation in the semi-infinite medium caused by the external radiation field $\psi_{\mathrm{inc}}(\boldsymbol{\rho}, \hat{\mathbf{s}}) = S(\boldsymbol{\rho})\delta(\hat{\mathbf{s}} - \hat{\mathbf{s}}_0)$, the radiance must satisfy the BC

$$\psi(\boldsymbol{\rho}, z=0, \hat{\mathbf{s}}) = \psi_{\mathrm{inc}}(\boldsymbol{\rho}, \hat{\mathbf{s}}) + R(\hat{\mathbf{s}}' \cdot \hat{\mathbf{n}})\psi(\boldsymbol{\rho}, z=0, \hat{\mathbf{s}}'), \quad \hat{\mathbf{s}} \cdot \hat{\mathbf{n}} < 0, \tag{40}$$

where $S(\boldsymbol{\rho})$ is an arbitrary function for describing the beam profile. By applying the two-dimensional Fourier transform Eq. (27), the BC becomes

$$\psi(\mathbf{q}, z=0, \hat{\mathbf{s}}) = \psi_{\mathrm{inc}}(\mathbf{q}, \hat{\mathbf{s}}) + R(\hat{\mathbf{s}}' \cdot \hat{\mathbf{n}})\psi(\mathbf{q}, z=0, \hat{\mathbf{s}}'), \quad \hat{\mathbf{s}} \cdot \hat{\mathbf{n}} < 0. \tag{41}$$

At this stage the principle procedure is the same as in the case for the isotropic point source inside the medium. However, here we must only consider the source free solution of the RTE. By substituting the homogeneous solution Eq. (20) in

the BC Eq. (41), multiplying both sides with $Y^*_{l'm'}(\hat{\mathbf{s}})$ and integrating over the hemisphere $\hat{\mathbf{s}}\cdot\hat{\mathbf{n}}<0$ results in the following set of linear equations:

$$\sum_{\lambda_i>0} C_i(\mathbf{q}) \sum_{l=\bar{l}}^{N} \psi_{lm'}(q\lambda_i) R^{m'}_{l'l} = S(\mathbf{q}) Y^*_{l'm'}(\hat{\mathbf{s}}_0) \exp(\mathrm{i}m'\phi_{\mathbf{q}}). \quad (42)$$

For the special case of a perpendicular incident beam with a rotationally symmetric profile function $S(\rho)=S(\rho)$, the system of linear equation becomes

$$\sum_{\lambda_i>0} C_i(q) \sum_{l=\bar{l}}^{N} \psi_{lm'}(q\lambda_i) R^{m'}_{l'l} = S(q)\sqrt{\frac{2l+1}{4\pi}}\delta_{m'0}, \quad (43)$$

where the constants $C_i(q)$ depend only on the length of the two-dimensional vector $\mathbf{q}$. Now we consider exactly the same linear independent equations from Eq. (31) labeled by l' and m' as before.

The spatially resolved reflectance caused by an external incident beam can also be obtained from Eq. (34) by using the BC Eq. (40) leading to

$$R(\rho) = \int (\hat{\mathbf{s}}\cdot\hat{\mathbf{n}})\psi(\rho, z=0, \hat{\mathbf{s}})\mathrm{d}^2 s - (\hat{\mathbf{s}}_0\cdot\hat{\mathbf{n}})S(\rho). \quad (44)$$

For the case of a perpendicular incident beam with $\hat{\mathbf{s}}_0=\hat{\mathbf{z}}$, we obtain the rotationally symmetric reflectance

$$R(\rho) = S(\rho) - \sqrt{\frac{4\pi}{3}}\psi^{(h)}_{10}(\rho, 0). \quad (45)$$

Finally, the fluence in the semi-infinite medium becomes the simple form

$$\Phi(\mathbf{r}) = \sqrt{4\pi}\psi^{(h)}_{00}(\rho, z). \quad (46)$$

3. NUMERICAL RESULTS

In this section the obtained general solution to the RTE is validated against the Monte Carlo method, which converges in the limit of an infinitely large number of simulated photons to the exact solution. For the following comparisons the Henyey–Greenstein phase function with $g=0.9$ is used. The optical properties of the scattering half-space medium is assumed to be $\mu_a = 0.01\ \mathrm{mm}^{-1}$ and $\mu_s = 10\ \mathrm{mm}^{-1}$, which are typical for biological tissue in the near-infrared spectral range. The refractive index of the nonscattering half-space is set to $n_{\mathrm{out}}=1.0$.

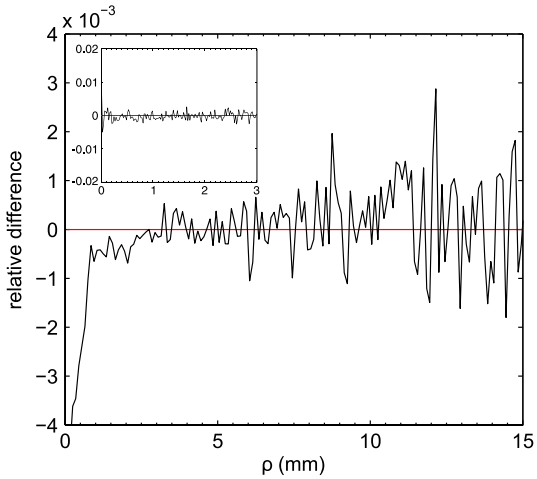

Fig. 2. (Color online) Relative differences between the analytical approach and the Monte Carlo simulation. The inset shows the relative differences for a higher spatial resolution within the Monte Carlo simulation and the radial distances $0\le\rho\le 3$ mm.

A. Reflectance

For the first comparison, we consider a isotropic point source inside the semi-infinite geometry, which is placed on the z axis at $z_0=l^*$, where $l^*=1/\sigma_1$ is the transport mean free path. The resulting reflected light from the boundary is computed with Eq. (44) and compared to the result obtained from the Monte Carlo method for matched and mismatched BCs; see Fig. 1.

Because of the small differences between the derived solution (solid curves) and the Monte Carlo simulation (symbols), we computed the relative error versus radial distance for the mismatched BC, which can be seen in Fig. 2.

The differences of the two solutions at small radial distances are due to the finite spatial resolution $\Delta x=\Delta y=$

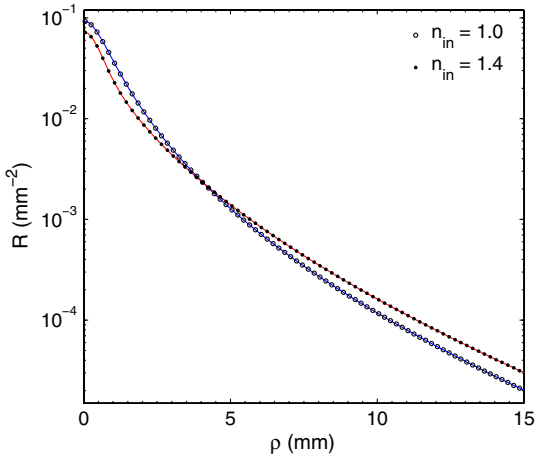

Fig. 1. (Color online) Spatially resolved reflectance caused by an isotropic point source located at $z_0=l^*$ inside the semi-infinite medium. The approximation order is $N=21$.

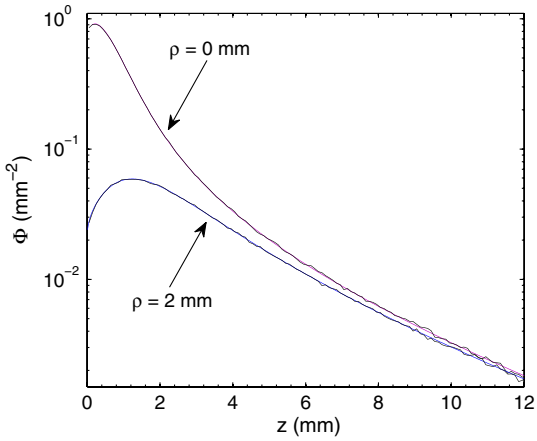

Fig. 3. (Color online) Fluence inside the semi-infinite medium with $n_{\mathrm{in}}=1.0$ caused by a Gaussian incident beam with radius $\eta=1$ mm. The approximation order is $N=13$.

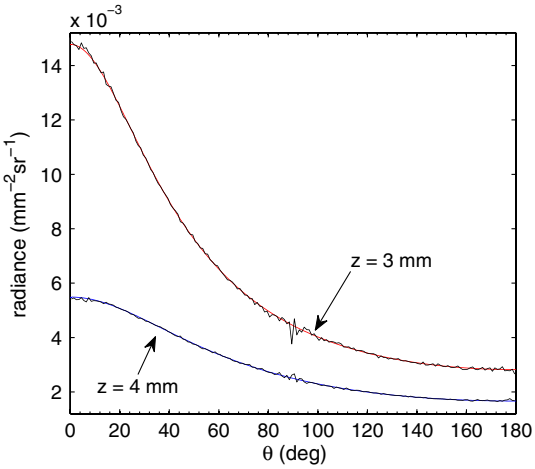

Fig. 4. (Color online) Angle-resolved Green's function for the RTE in the semi-infinite geometry caused by a perpendicular incident δ beam. The approximation order is $N = 13$.

0.1 mm used in the Monte Carlo simulation. This error can be arbitrarily reduced by decreasing the spatial grid as is shown in the inset of Fig. 2, where $\Delta x = \Delta y = 0.02$ mm was used.

The obtained analytical reflectance from the semi-infinite medium agrees with the result from the Monte Carlo method for both matched and mismatched BCs.

B. Fluence

The fluence caused by an external radiation field of the form

$$\psi_{\mathrm{inc}}(\boldsymbol{\rho}, \hat{\mathbf{s}}) = \frac{2}{\pi\eta^2} \exp\left(\frac{2\rho^2}{\eta^2}\right)\delta(\hat{\mathbf{s}} - \hat{\mathbf{z}}) \tag{47}$$

within the half-space medium is computed by the analytical Eq. (46) and the Monte Carlo method for two different radial distances. Here η denotes the radius of the Gaussian beam. The corresponding results are shown in Fig. 3.

As in the case for the reflectance, the derived analytical expression (smooth curves) and the Monte Carlo simulation (noisy curves) lead practically to the same fluence.

C. Radiance

The Green's function for the RTE in the semi-infinite geometry caused by the perpendicular incident δ beam

$$\psi_{\mathrm{inc}}(\boldsymbol{\rho}, \hat{\mathbf{s}}) = \delta(\boldsymbol{\rho})\delta(\hat{\mathbf{s}} - \hat{\mathbf{z}}) \tag{48}$$

is computed according to Eq. (22) and with the Monte Carlo method for $n_{\mathrm{in}} = 1.0$. The resulting radiance is evaluated for two different detector positions at the z axis and is shown in Fig. 4 as function of the polar angle θ.

The analytical Green's function for the radiance (smooth curves) also agrees to the radiance as simulated with the Monte Carlo method (noisy curves) within the statistical errors of the simulations.

4. CONCLUSIONS

In this study the three-dimensional RTE is solved for the boundary-value problem in the semi-infinite geometry including the effect of Fresnel reflection at the interface. The obtained general solution to the homogenous RTE has an analytical dependence on the spatial and angular variables. The unknown constants result from the solution of a system of linear equations that arises from the corresponding BC. Apart from the truncation of the applied spherical harmonics expansions, the derivations contain no approximations and/or are not based on simplified assumptions for obtaining the general solution to the homogeneous RTE.

The derived solutions were compared to Monte Carlo simulations for the reflectance, fluence, and radiance considering external and internal sources. The differences of the results obtained by both methods were within the statistics of the Monte Carlo method.

Besides the direct application of the derived equations for a variety of problems in different scientific fields, another important point is the validation of numerical methods for solving the RTE such as the Monte Carlo simulation. Especially for the numerical solution of the spherical harmonics equations, also called the P_N approximation, the derived analytical equations can be used to estimate the accuracy of the applied approximation order N.

APPENDIX A: NUMERICAL PROCEDURE

This appendix contains the complete numerical procedure divided into six steps for obtaining the general solution to the homogeneous RTE in cases when the radiance takes the form $\psi(\mathbf{r}, \hat{\mathbf{s}}) = \psi(\rho, z, \theta, \chi)$.

Step 1. Compute the coefficients $R_{ll}^{m'}$ for the values $l' = m' + 1,\ m' + 3, \ldots, N$, and $m' \le l \le N$, where $m' = 0, \ldots, N - 1$, according to Eq. (32).

Step 2. Perform the EVD of the matrices $\mathbf{B}_M$ from Eq. (12) for $M = 0, 1, \ldots, N - 1$, which gives all in all $(N + 1)^2/4$ eigenvalues $\lambda_i > 0$ together with the corresponding eigenvectors $|\nu_i\rangle$ having components $\langle l|\nu_i\rangle$, where $M \le l \le N$. Note that the eigenvalues $\lambda_i \le 0$, which also appear within the EVD, are excluded from the solution. The EVD for the value $M = N - 1$ can be directly performed, leading to the eigenvalue $\lambda = 1/\sqrt{(2N + 1)\sigma_{N-1}\sigma_N}$ and the eigenvector components $\langle N - 1|\nu\rangle = \langle N|\nu\rangle = 1/\sqrt{2}$. Regarding Steps 4 and 5, it would be advantageous here to provide the mapping $f : \lambda \mapsto M$. In other words, we must keep in mind which eigenvalues λ_i follows from the EVD of which matrix $\mathbf{B}_M$.

Step 3. In this step, the Wigner d functions are evaluated as a function of the transform variable q by using the recursively defined algorithm reported in [18]. To this end, we define five start values, namely $d_{00}^0[\theta_{\mathbf{k}}(q\lambda)] = 1$ and

$$\begin{aligned} d_{00}^1[\theta_{\mathbf{k}}(q\lambda)] &= -\sqrt{1 + (q\lambda)^2}, \\ d_{10}^1[\theta_{\mathbf{k}}(q\lambda)] &= -\mathrm{i}\frac{q\lambda}{\sqrt{2}}, \\ d_{11}^1[\theta_{\mathbf{k}}(q\lambda)] &= \frac{1 - \sqrt{1 + (q\lambda)^2}}{2}, \\ d_{1,-1}^1[\theta_{\mathbf{k}}(q\lambda)] &= \frac{1 + \sqrt{1 + (q\lambda)^2}}{2}. \end{aligned} \tag{A1}$$

The following procedure written in italic text must be performed successively for each value $l = 2, 3, \ldots, N$ in upward direction.

Compute the Wigner d functions for all $m = 0, \ldots, l - 2$ *and* $|M| \le m$ *according to the recurrence*

$$d^l_{mM} = \frac{l(2l-1)}{\sqrt{(l^2-m^2)(l^2-M^2)}}\left[\left(d^1_{00} - \frac{mM}{l(l-1)}\right)d^{l-1}_{mM} - \frac{\sqrt{[(l-1)^2-m^2][(l-1)^2-M^2]}}{(l-1)(2l-1)}d^{l-2}_{mM}\right]. \quad \text{(A2)}$$

After that, evaluate the relations

$$d^l_{l-1,l-1} = (1-l+ld^1_{00})d^{l-1}_{l-1,l-1}, \quad \text{(A3)}$$

$$d^l_{ll} = d^1_{11}d^{l-1}_{l-1,l-1}. \quad \text{(A4)}$$

Next, for $M = l, l-1, \ldots, 1-l$ *making use of the recurrence*

$$d^l_{l,M-1} = \sqrt{\frac{l+M}{l-M+1}}\frac{\mathrm{i}q\lambda}{\sqrt{1+(q\lambda)^2}-1}d^l_{l,M}, \quad \text{(A5)}$$

and for $M = l-1, l-1, \ldots, 2-l$ *of*

$$d^l_{l-1,M-1} = \frac{ld^1_{00}-M+1}{ld^1_{00}-M}\sqrt{\frac{l+M}{l-M+1}}\frac{\mathrm{i}q\lambda}{\sqrt{1+(q\lambda)^2}-1}d^l_{l-1,M}, \quad \text{(A6)}$$

replace l *by* $l+1$ *and repeat the procedure written in italic text until the final value* $l = N$ *is reached.*

Finally, for every value $l = 1, 2, \ldots, N$, evaluate the two symmetry properties

$$d^l_{Mm} = (-1)^{m+M}d^l_{mM}, \quad \text{(A7)}$$

$$d^l_{M,-m} = d^l_{m,-M}, \quad \text{(A8)}$$

for all $m = 1, \ldots, l$ and $M = 0, \ldots, m-1$ to find the remaining Wigner d functions. The closed-form expression Eq. (19) can be used for checking results obtained by the above recursively defined algorithm.

Step 4. For every eigenvalue λ_i, compute the kernels $\psi_{lm}(q\lambda_i)$ according to Eq. (21), where $M \le l \le N$ and $0 \le m \le l$. For finding the correct value M, we remember on the function $M = f(\lambda)$ from Step 2. At this stage the general solution Eq. (20) to the homogeneous RTE Eq. (3) is given in terms of analytical functions.

Step 5. Compute the unknown constants $C_i(q)$, which appears in the homogeneous solution Eq. (22), by solving a system of $(N+1)^2/4$ linearly independent equations, which follows from the corresponding BC. The principle procedure is analogous to that as already shown in Subsection 2.B. For every value $m' = 0, \ldots, N-1$ compute the pairs (l', m'), where $l' = m'+1,\ m'+3, \ldots, N$. Then use all linear equations labeled by the above computed pairs.

Step 6. For obtaining the general solution Eq. (22) in real space, we must calculate the corresponding kernels $\psi_{lm}(\rho, z)$ via numerical integration according to the inverse Hankel transform Eq. (23). This fact entails that Steps 3–5 must be performed for every value of the transform variable q, which becomes a finite number of discretization points q_j within the numerical implementation. Note that the Wigner d functions regarding the angular dependence within Eq. (22) can also be expanded in terms of associated Legendre polynomials

$$d^l_{m0}(\theta) = \sqrt{\frac{(l-m)!}{(l+m)!}}P^m_l(\cos\theta). \quad \text{(A9)}$$

ACKNOWLEDGMENTS

We acknowledge the support by the European Union (nEUROPt, grant agreement no. 201076).

REFERENCES

1. K. M. Case and P. F. Zweifel, *Linear Transport Theory* (Addison-Wesley, 1967).
2. E. D'Eon and G. Irving, "A quantized-diffusion model for rendering translucent materials," ACM Trans. Graph. **30**, 56:1–56:12 (2011).
3. A. Ishimaru, *Wave Propagation and Scattering in Random Media* (Academic, 1978).
4. A. Kienle and R. Hibst, "Light guiding in biological tissue due to scattering," Phys. Rev. Lett. **97**, 018104 (2006).
5. B. Wilson and G. Adam, "A Monte Carlo model for the absorption and flux distributions of light in tissue," Med. Phys. **10**, 824–830 (1983).
6. F. Martelli, S. Del Bianco, A. Ismaelli, and G. Zaccanti, *Light Propagation Through Biological Tissue* (SPIE, 2010).
7. P. S. Mohan, T. Tarvainen, M. Schweiger, A. Pulkkinen, and S. R. Arridge, "Variable order spherical harmonic expansion scheme for the radiative transport equation using finite elements," J. Comput. Phys. **230**, 7364–7383 (2011).
8. A. H. Hielscher, R. E. Alcouffe, and R. L. Barbour, "Comparison of finite-difference transport and diffusion calculations for photon migration in homogeneous and heterogeneous tissues," Phys. Med. Biol. **43**, 1285–1302 (1998).
9. B. D. Ganapol, "Radiative transfer with internal reflection via the converge discrete ordinates method," J. Quant. Spectrosc. Radiat. Transfer **112**, 693–713 (2011).
10. M. M. R. Williams, "The searchlight problem in radiative transfer with internal reflection," J. Phys. A Math. Theor. **40**, 6407–6425 (2007).
11. V. A. Markel, "Modified spherical harmonics method for solving the radiative transport equation," Waves Random Complex Media **14**, L13–L19 (2004).
12. A. Liemert and A. Kienle, "Radiative transfer in two-dimensional infinitely extended scattering media," J. Phys. A Math. Theor. **44**, 505206 (2011).
13. G. Panasyuk, J. C. Schotland, and V. A. Markel, "Radiative transport equation in rotated reference frames," J. Phys. A Math. Gen. **39**, 115–137 (2006).
14. M. Machida, G. Y. Panasyuk, J. C. Schotland, and V. A. Markel, "The Green's function for the radiative transport equation in the slab geometry," J. Phys. A Math. Theor. **43**, 065402 (2010).
15. A. Liemert and A. Kienle, "Analytical approach for solving the radiative transfer equation in two-dimensional layered media," J. Quant. Spectrosc. Radiat. Transfer **113**, 559–564 (2012).
16. A. Liemert and A. Kienle, "Green's functions for the two-dimensional radiative transfer equation in bounded media," J. Phys. A Math. Theor. **45**, 175201 (2012).
17. S. R. Arridge, "Optical tomography in medical imaging," Inverse Probl. **15**, R41–R93 (1999).
18. M. A. Blanco, M. Flórez, and M. Bermejo, "Evaluation of the rotation matrices in the basis of real spherical harmonics," J. Mol. Struct. **419**, 19–27 (1997).
19. N. Baddour, "Operational and convolution properties of two-dimensional Fourier transforms in polar coordinates," J. Opt. Soc. Am. A **26**, 1767–1777 (2009).
20. M. M. R. Williams, "The Milne problem with Fresnel reflection," J. Phys. A Math. Gen. **38**, 3841–3856 (2005).